A Generalized Turbulent Dispersion Model for bubbly flow numerical simulation in NEPTUNE_CFD

J. Laviéville, N. Mérigoux, M. Guingo, C. Baudry, S. Mimouni
Electricité de France, R&D Division
6 Quai Watier, 78401 Chatou, France
jerome-marcel.lavieville@edf.fr

ABSTRACT

The NEPTUNE_CFD code, based upon an Eulerian multi-fluid model, is developed within the framework of the NEPTUNE project, financially supported by EDF (Electricité de France), CEA (Commissariat à l'Energie Atomique et aux Energies Alternatives), IRSN (Institut de Radioprotection et de Sûreté Nucléaire) and AREVA-NP. NEPTUNE_CFD is mainly focused on Nuclear Safety applications involving two-phase water-steam flows, like two-phase Pressurized Shock (PTS) and Departure from Nucleate Boiling (DNB).
Many of these applications involve bubbly flows, particularly, for application to flows in PWR fuel assemblies, including studies related to DNB.

Considering a very usual model for interfacial forces acting on bubbles, including drag, virtual mass and lift forces, the Turbulent Dispersion Force is often added to moderate the lift effect in orthogonal directions to the main flow and get the right dispersion shape.

This paper presents a formal derivation of this force, considering on the one hand, the fluctuating part of drag and virtual mass, and on the other hand, Turbulent Pressure derivation obtained by comparison between Lagrangian and Eulerian description of bubbles motion. An extension of the Tchen's theory is used to express the turbulent kinetic energy of bubbles and the two-fluid turbulent covariance tensor in terms of liquid turbulent velocities and time scale. The model obtained by this way, called Generalized Turbulent Dispersion Model (GTD), does not require any user parameter.

The model is validated against Liu & Bankoff air-water experiment, Arizona State University (ASU) experiment, DEBORA experiment and Texas A&M University (TAMU) boiling flow experiments.

KEYWORDS: Two phase Bubbly Flow, Turbulent Dispersion, Validation, DNB.

1. INTRODUCTION

The NEPTUNE_CFD code developed in the framework of the NEPTUNE project [1] is mainly focused on Nuclear Reactor Safety applications involving two-phase flows, as for example, two-phase Pressurized Thermal Shock (PTS) and Departure from Nucleate Boiling (DNB). Since the maturity of two-phase CFD has not reached yet the same level as single phase CFD, an important work of model development and thorough validation is needed. Many of these applications involve bubbly and boiling flows, and therefore it is essential to validate the software on such configurations. In particular, this is crucial for applications to flows in PWR fuel assemblies, including studies related to DNB.
During the last decade, important work has been performed on this topic, including second-order two-phase turbulence prediction and induced turbulence[2,3,4], prediction of interfacial area, specific two-

phase wall functions, forces acting on bubbles, poly-dispersion [5,6], and of course validation on various configurations. Today, we are aware that the turbulent dispersion is a key point of the physical modeling.
In the first part of this paper, we present the derivation of the turbulent dispersion force that can be seen as the turbulent contribution on forces acting on local bubbles. The main idea is to derive Eulerian equations from a Lagrangian description of bubbles and on the carrier fluid (liquid).
In the second part, we compare our model with other classical formulations of the turbulent dispersion force, one proposed by Lopez de Bertodano [7], the other one obtained by Burns[8]. Models are compared using 7 test-cases of the NEPTUNE_CFD validation database.

2. MODEL DESCRIPTION

2.1. Two-phase basic solver and model

NEPTUNE_CFD is a three dimensional two-fluid code mainly developed for nuclear reactor applications. The associated model is an extension of the classical two-fluid one-pressure approach [9, 2]. It simulates multi-component multiphase flows, solving a set of three balance equations for each field [10, 2].
The discretization is based on a 3D full-unstructured finite-volume approach, with a collocated arrangement of all variables. Numerical consistency and precision for diffusive and advective fluxes are taken into account through a gradient reconstruction technique, for non-regular cells. Convective schemes for all variables, except pressure, are centered / upwind scheme.
The solver is based on a pressure correction fractional step approach associated to an iterative procedure that leads to mass, energy and total volume conservation.
Local balance equations for mass, momentum and energy are written for each phase. These balance equations are obtained by ensemble averaging the local instantaneous balance equations written for each phase that take into account interfacial mass, energy and momentum transfers.
Additional conservation equations are written for turbulence and interfacial area closures.
A full and closed set of models and closures has been chosen for the simulation of two-phase bubbly flows, without any adjustable user parameters. It is used for the whole set of validation test-cases.
It includes momentum interfacial transfer closures: Ishii drag force, Zuber virtual mass force, Tomiyama lift and wall Lubrication forces, and Turbulent Dispersion force that will be discussed later.
Bulk mass and energy transfer uses Manon-Berne model [11] while bubble nucleation at heated walls uses an extension of Kurul-Podowski heat partitioning model. Second-order turbulence is predicted using the SSG Rij-epsilon including bubbles turbulence production. Interfacial area transport equation, based on the Ruyer-Seiler polydispersed formulation and taking into account coalescence and break-up is systematically used to predict local bubble sizes [5, 6].

NEPTUNE_CFD inherits the I/O and High Performance Computing capabilities of the EDF open-source CFD software *Code_Saturne* used as a pre-requisite library, can be coupled with the SYRTHES solid-conduction code for conjugate heat transfer and can be used as a module of the SALOME plate-form.

2.2. Previous closures of the Turbulent Dispersion Force

Turbulence dispersion force mainly results in dispersion of bubbles from high to low volume fraction regions due to liquid turbulent fluctuations. This contribution is supposed to balance the lift and drag effect in radial direction to the flow.

Lopez de Bertodano [7] first proposed to model this contribution by taking into account the local turbulence intensity. He writes:

$$F^{TD} = -Ctd\rho_1 k_1 \nabla \alpha_2 \tag{1}$$

with ρ_1 and k_1 the density and turbulent kinetic energy of liquid, α_2 the void fraction.

Here Ctd is an adjustable user parameter with default value equal to 0.1. Nevertheless, the author has shown that a drastic increase of the parameter is necessary (up to 500) to get acceptable results [38]. This model was historically the first one implemented in NEPTUNE_CFD.

More recently, Burns et al. [8] derived an expression averaging the drag force contribution, considering the dominant combined action of turbulent eddies and drag : dispersed particles get caught up in continuous phase turbulent eddies, and are transported by the effect of interphase drag. The model writes:

$$F^{TD} = -\alpha_2 C_D \frac{\nu_1^t}{\sigma^t}\left(\frac{\nabla \alpha_2}{\alpha_2} - \frac{\nabla \alpha_1}{\alpha_1}\right) \tag{2}$$

With C_D the interfacial drag coefficient, α_1 and ν_1^t the liquid volume fraction and turbulent viscosity, and σ^t a turbulent Schmidt number equal to 0.9. Following the authors, this model is supposed to cover a large range of flow without needing adjustable constant.

In the next section, we will test these models on the NEPTUNE_CFD bubbly-flow validation database.

2.3. Generalized Turbulent Dispersion derivation: from Lagrangian to Eulerian formulation.

This work is based in the one hand on a large number of research made at EDF R&D by Simonin et al. [12, 13, 14, 15, 33, 34] on the dispersion of heavy or light particles in stationary isotropic or simple shear turbulent flow, and on the other hand, on the work of J.P. Minier & E. Peirano [16, 36] on a stochastic approach for modeling and simulation of polydispersed multiphase flows.

2.3.1. Lagrangian equation for bubble motion

The main initial idea is a Lagrangian description of the dispersed phase (particles or bubbles)

$$\rho_2 \frac{du_2}{dt} = F_2^{\ p} + F_2^{\ np} + \rho_2 g \tag{3}$$

In Eq. 3, $F_2^{\ p}$ denotes the force acting on the particle by a continuous fluid. It can be decomposed, following Maxey-Riley [35] and Gatignol [17] on drag and virtual mass contributions. Since bubbly flow are involved, it seems relevant here to add the lift contribution

$$F_2^{\ p} = \rho_1 F_D(\tilde{u}_1 - u_2) + \rho_1 C_{VM}\left(\frac{D\tilde{u}_1}{Dt} - \frac{du_2}{dt}\right) + \rho_1 C_L \Omega \otimes (\tilde{u}_1 - u_2) \tag{4}$$

F_D , C_{VM} C_L are drag, virtual mass and lift coefficient (closure used in NEPTUNE_CFD can be found in [18, 19]). Ω denotes the liquid vorticity (or rotational). $\tilde{u}_1$ is the local surrounding liquid velocity, which can be obtained by extrapolation procedure on the particle volume center.

$F_2^{\ np}$ is the force applied by the locally undisturbed continuous field, which can be associated to a pressure contribution. For very low Stokes number, Gatignol takes into account the continuous phase acceleration. Simonin et al. generalize this approach to larger Stokes number and obtain:

$F_2^{\ p} = \rho_1\left(\frac{D\tilde{u}_1}{Dt} - g\right)$ with $\frac{D}{Dt} = \frac{\partial}{\partial t} + u_2 \nabla$ the Lagrangian derivative along particle trajectory.

In the end, the particle Lagrangian equation writes:

$$\frac{du_2}{dt} = \frac{\tilde{u}_1 - u_2}{\tau_{12}^F} + b\frac{D\tilde{u}_1}{Dt} + c\Omega(\tilde{u}_1 - u_2) + eg, \qquad D\tilde{u}_1 = \tilde{u}_1(x + u_2 dt, t + dt) - \tilde{u}_1(x,t) \tag{5}$$

$$\text{with } \tau_{12}^F = F_D^{-1}\left(\frac{\rho_2}{\rho_1} + C_{VM}\right), b = \frac{\rho_1 + \rho_1 C_{VM}}{\rho_2 + \rho_1 C_{VM}}, c = \frac{\rho_1 C_L}{\rho_2 + \rho_1 C_{VM}}, e = \frac{\rho_2 - \rho_1}{\rho_2 + \rho_1 C_{VM}} \tag{6}$$

2.3.2. Langevin equation for liquid velocity along bubble trajectories.

Following Simonin et al. and Minier et al. works, the fluid acceleration along particle trajectory is modeled by using a Langevin [20] equation. For high Reynolds number, it writes:

$$D\tilde{u}_{1,i} = -\frac{1}{\rho_1}\frac{\partial P}{\partial x_i}dt + \left[u_{2,j} - \tilde{u}_{1,j}\right]\frac{\partial U_{1,i}}{\partial x_j}dt + G_{12,ij}[\tilde{u}_{1,j} - U_{1,j}]dt + C_{12}dW_{12,i} \tag{7}$$

$U_{1,i}$ is the mean liquid velocity, W_{12} is the Wiener stochastic process, and G_{12} a dispersion tensor that can be considered isotropic in first approximation: $G_{12,ij} = -\frac{\delta_{ij}}{\tau_{12}^t}$.

τ_{12}^t is the Lagrangian time scale of the fluid turbulence along particle trajectories defined by $\tau_{12}^t = \frac{1}{\left\langle u_{1,i}'(t)u_{1,i}'(t)\right\rangle_2}\int_0^\infty \left\langle u_{1,i}'(t)u_{1,i}'(t+\tau)\right\rangle_2 d\tau$.

It can be estimated from two-fluid Lagrangian simulations. Csanady [21], Deutsch and Simonin [13] have shown that this integral time scale can be very different from fluid turbulence characteristic time scales and modeled it using the so-called crossing trajectory effect:

$$\tau_{12}^t = \frac{3}{2}C_\mu \frac{k_1}{\varepsilon_1}\left(1 + \beta\frac{V_r^2}{k_1}\right)^{-\frac{1}{2}}, \beta = 2.7 \tag{8}$$

2.3.3. From two-phase velocity distribution evolution to Eulerian equations

Still following the methodology of Simonin et al. and Minier et al., we can derive from Lagrangian equations (5) and (7) a more general Fokker-Planck-type equation describing the evolution of the joint two-phase velocity distribution $f_{12}(c_f, c_p, x, t)$ giving the probable number of bubbles per unit volume located at position x and time t with c_p and c_f bubble and liquid ("seen" by bubbles) velocities.

Integrating the Fokker-Planck equation upon the two-phase velocity sample space, any transport equation for the statistic average of a function Ψ (function of c_f, c_p, x and t) can then be obtained and takes the general form:

$$\begin{aligned}
&\frac{\partial}{\partial t}\alpha_2\rho_2\langle\Psi\rangle + \frac{\partial}{\partial x_i}\alpha_2\rho_2\langle c_{p,i}\Psi\rangle = \alpha_2\rho_2\left\langle\left(\left(\frac{\delta_{ij}}{\tau_{12}^F} + c\Omega_{ij}\right)\left(c_{f,j} - c_{p,j}\right) + eg_i\right)\frac{\partial\Psi}{\partial c_{p,i}}\right\rangle \\
&+ \alpha_2\rho_2\left\langle\left(-\frac{1}{\rho_1}\frac{\partial P}{\partial x_i} + \left(c_{p,j} - c_{f,j}\right)\frac{\partial U_{1,i}}{\partial x_j} + G_{12,ij}\left(c_{f,j} - U_{1,j}\right)\right)\left(\frac{\partial\Psi}{\partial c_{f,i}} + b\frac{\partial\Psi}{\partial c_{p,i}}\right)\right\rangle \\
&+ \alpha_2\rho_2\left\langle\frac{\partial\Psi}{\partial t} + c_{p,i}\frac{\partial\Psi}{\partial x_i}\right\rangle \quad + \frac{1}{2}\alpha_2\rho_2 C_{12}^2\left(\left\langle\frac{\partial^2\psi}{\partial c_{f,m}\partial c_{f,m}} + 2b\frac{\partial^2\psi}{\partial c_{f,m}\partial c_{p,m}} + b^2\frac{\partial^2\psi}{\partial c_{p,m}\partial c_{p,m}}\right\rangle\right)
\end{aligned} \tag{9}$$

In the following, $\langle\ \rangle$ denotes the statistical mean upon bubbles distribution.

Taking $\Psi = c_p$ in equation (9), and considering formula (6) and equation (4), we get rigorously the bubble mean velocity equation, $\langle\Psi\rangle = U_2$:

$$\begin{aligned}\frac{\partial}{\partial t}\alpha_2\rho_2 U_{2,i} + \frac{\partial}{\partial x_j}\alpha_2\rho_2 U_{2,j}U_{2,i} + \frac{\partial}{\partial x_j}\alpha_2\rho_2\langle u'_{2,i}\,u'_{2,j}\rangle &= -\alpha_2\rho_2\frac{\partial P}{\partial x_i} + \rho_2 g_i - \alpha_2\rho_1\frac{\langle u'_{1,i}\rangle}{\tau_{12}^t} \\ &\quad -\alpha_2\rho_1\langle F_D\rangle\left(U_{2,i} - U_{1,i} - \langle u'_{1,i}\rangle\right) - \alpha_2\rho_1\langle C_L\rangle\Omega_{ij}\left(U_{2,j} - U_{1,j} - \langle u'_{1,j}\rangle\right) \\ -\rho_1\langle C_{VM}\rangle\left[\alpha_2\left(\frac{\partial}{\partial t} + U_{2,j}\frac{\partial}{\partial x_j}\right)\left(U_{2,i} - U_{1,i}\right) + \frac{\partial}{\partial x_j}\left(\alpha_2\left(\langle u'_{2,i}\,u'_{2,j}\rangle - \langle u'_{1,i}\,u'_{2,j}\rangle\right)\right)\right]\end{aligned} \tag{10}$$

This transport equation introduces the so-called turbulent pressure contribution (last term of line 1), the so-called drift velocity $\langle u'_{1,i}\rangle$ (mean liquid velocity fluctuations along bubble trajectories) and a turbulent virtual mass contribution (last term of the third line). The drift velocity equation can rigorously be obtained taking $\Psi = c_f - U_1$ in equation (9) and using the single-phase liquid momentum transport equation. Neglecting mean velocity gradient and time derivative, the term writes:

$$\langle u'_{1,i}\rangle = -\tau_{12}^t\left(\frac{1}{\alpha_2\rho_2}\frac{\partial}{\partial x_j}\alpha_2\rho_2\langle u'_{1,i}\,u'_{2,j}\rangle - \frac{1}{\alpha_1\rho_1}\frac{\partial}{\partial x_j}\alpha_1\rho_1\langle u'_{1,i}\,u'_{1,j}\rangle\right) \tag{11}$$

Finally, under same homogeneous flow hypothesis; algebraic relations between the bubble diagonal component of the Reynolds stresses $\langle u'_{2,i}\,u'_{2,i}\rangle$, the liquid-bubbles fluctuating velocity covariance tensor $\langle u'_{1,i}\,u'_{2,i}\rangle$, and the liquid Reynolds stresses "viewed" by the bubbles (at the location of the bubbles) can be obtained, taking $\Psi = (c_{f,i} - U_{1,i})(c_{f,i} - U_{1,i})$, $\Psi = (c_{f,i} - U_{1,i})(c_{p,i} - U_{2,i})$ and $\Psi = (c_{p,i} - U_{2,i})(c_{p,i} - U_{2,i})$ in equation (9) (see Minier-Peirano) :

$$\langle u'_{1,i}\,u'_{2,i}\rangle = \frac{b+\eta_r}{1+\eta_r}\langle u'_{1,i}\,u'_{1,i}\rangle \quad \langle u'_{2,i}\,u'_{2,i}\rangle = \frac{b^2+\eta_r}{1+\eta_r}\langle u'_{1,i}\,u'_{1,i}\rangle \quad \text{with } \eta_r = \frac{\tau_{12}^t}{\tau_{12}^F} \tag{12}$$

These relations generalize those obtained by Tchen [22] and Hinze [23], working on dispersion of very small particles in an isotropic and homogeneous turbulence.

2.3.4. Final closure for the generalized turbulent dispersion force

In equation (10), one can recognize classical contribution for drag, virtual mass and lift, function of mean velocities U_1 and U_2 and mean transfer coefficients.

Neglecting gradient of velocity fluctuations and identifying the liquid stresses viewed by the bubbles to the liquid stresses, the remaining fluctuating contribution gives the generalized turbulent dispersion force:

$$\boxed{F^{TD} = -GTD\rho_1 k_1 \nabla\alpha_2\,, \quad \text{with } GTD = \left(\langle F_D\rangle\tau_{12}^t - 1\right)\frac{b+\eta_r}{1+\eta_r} + \langle C_{VM}\rangle\frac{b^2+\eta_r}{1+\eta_r}} \tag{13}$$

3. NEPTUNE_CFD VALIDATION – DISPERSION MODELS COMPARISON

In this section, we present the comparison between measures and numerical simulations obtained on the basis of 7 cases of validation from the NEPTUNE_CFD validation database.
First simulations are adiabatic. They involve either liquid-water-air bubbles flow (Liu-Bankoff experiments and Bel F'dhila experiment), or water-freon flow (CHAPTAL experiment). The following ones involve boiling refrigerant flows at relatively low Reynolds number (ASU experiment and TAMU experiment) and high Reynolds number (DEBORA experiment), and one water-steam flow at high pressure and temperature (Bartolomei experiment).
For each simulation, we present a comparison of available experimental data (void fraction, velocity fields, temperature, turbulence, interfacial area) with several numerical results obtained with NEPTUNE_CFD, using the Generalized Turbulent Dispersion model, Burns model, Lopez de Bertodano model (for two chosen values of the user constant). In all the following figures the three models are presented under the names "GTD model", "Burns model" and "LdB Ctd =value". Corresponding curves are respectively black red and green.
The other closures models (interfacial mass, momentum and energy, use of a transport equation for the interfacial area, turbulence model SSG-Rij-epsilon taking into account the turbulent reverse coupling) are kept unchanged.
All the results presented correspond to converged steady states. Temporal convergence has been checked.
Mesh convergence has been checked for all cases of validation using three mesh-refinements in the radial direction, resp. 20, 40 and 80 cells. Results obtained with the finest meshes are presented here.
All the computational geometries are 2D-sector except for TAMU experiment which is simulated using a full rectangular 3D mesh.
Experimental uncertainties are not plotted since the purpose of the paper is to assess the sensitivity to the dispersion model.

3.1. Adiabatic validation test-cases

3.1.1. Liu-Bankoff test-case

This test case features an upward bubbly flow in a circular pipe. It represents a water / air two-phase flow with a low void fraction. The flow is isothermal, incompressible and turbulent with a Reynolds Number equal to 47000. This configuration has been studied experimentally by Liu and Bankoff [24]. Previous results with NEPTUNE_CFD has been obtained by Mimouni et al. [3].The test case section is a 2800 mm long, vertical smooth acrylic tubing, with inner diameter of 38 mm. Bubbles are produced by injecting air into a bundle of 64 equally-spaced 0.1 mm needles. In the selected experimental test case, the bubble diameter is equal to 2.5 mm. The void fraction at the inlet is 0.045. At the inlet, the water mean axial velocity is equal to 1.138 m/s and the gas mean axial velocity is equal to 1.33 m/s.

Figure 3.1 presents comparisons for liquid velocity, void fraction, gas velocity, fluctuating velocities for liquid (in axial and radial directions) and gas (in axial direction), liquid turbulent shear stress, at the end of the test section. X axis denotes the radial coordinate (in m); wall is on the right side.
The last graph presents comparisons of the turbulent dispersion force coefficient, extracted from the different models (equal to Ctd for Lopez de Bertodano) model.
GTD and Burns model show comparable behavior even if the associated turbulent coefficients are different, which means that, for this regime, the void fraction distribution is relatively insensitive to the radial distribution of Ctd. Near the wall, the void fraction peak level is well reproduced by Lopez de Bertodano model, using the recommended value.
Liquid Radial and axial velocity fluctuations are correctly predicted. The good level prediction of the axial bubble velocity fluctuation validates equation (12).

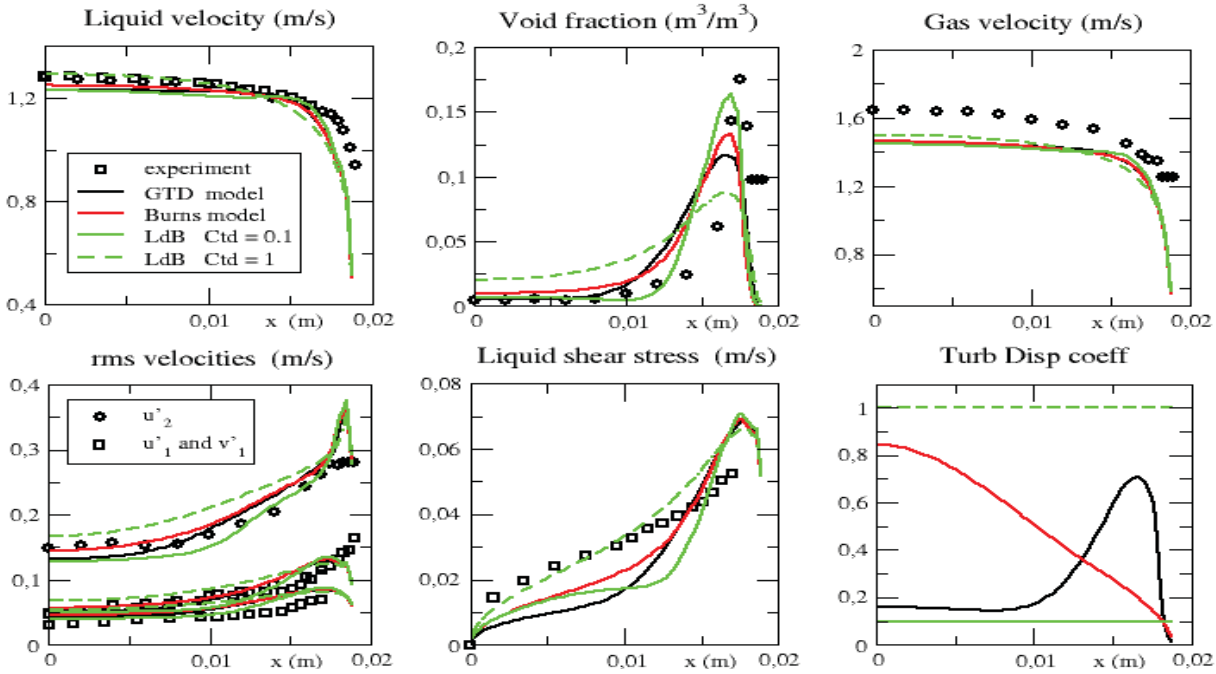

Figure 3-1.1 Liu-Bankoff experiment. Comparison of experimental data and NEPTUNE_CFD simulations for GTD, Burns and Lopez de Bertodano dispersion models.

3.1.2. Bel F'dhila and Simonin sudden expansion experiment [25]

This test case features a two-phase bubbly flow in vertical cylindrical pipe, in the presence of a sudden expansion. It concerns a water / air two-phase flow with a high void fraction (over 10 %) and Reynolds Number around 10^5. The flow is isothermal, incompressible and turbulent. This configuration has been studied experimentally and numerically by Bel F'Dhila and Simonin [25, 26, 27].

Measurements were performed for averaged velocity and turbulent quantities of the fluid and for the void fraction.

The experimental facility consists of two vertical pipes of 50 and 100 mm diameters with an overall height of 340 mm. The abrupt expansion is located at 20 mm from the air-water inlet section. It induces recirculation and redistribution of bubbles under the combined action of the turbulent mixing and the influence of gravity. Air is injected in the nozzle of a Venturi through an annular slot producing millimeter bubbles.

Figure 3.1-2 presents comparisons for void fraction, mean and fluctuating liquid velocities for two selected height of the test-section, Z=0.18 and Z=0.32m. X axis denotes the radial coordinate (in m).

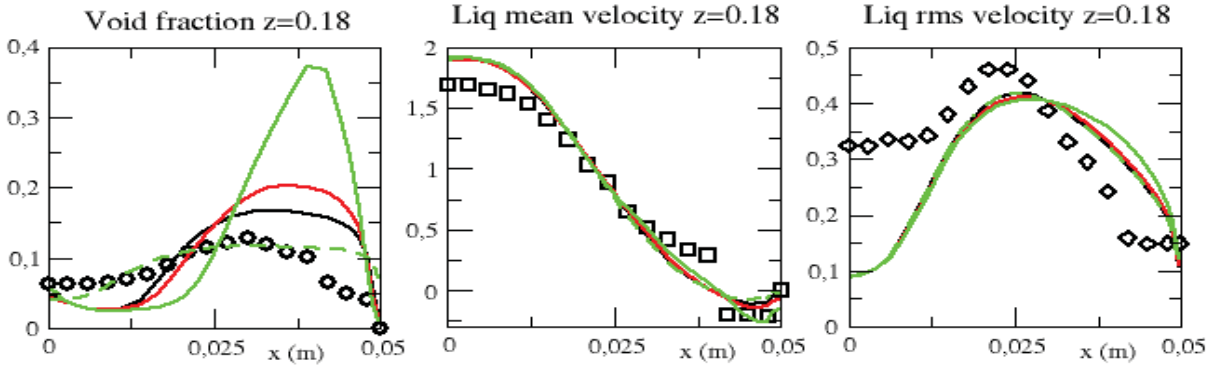

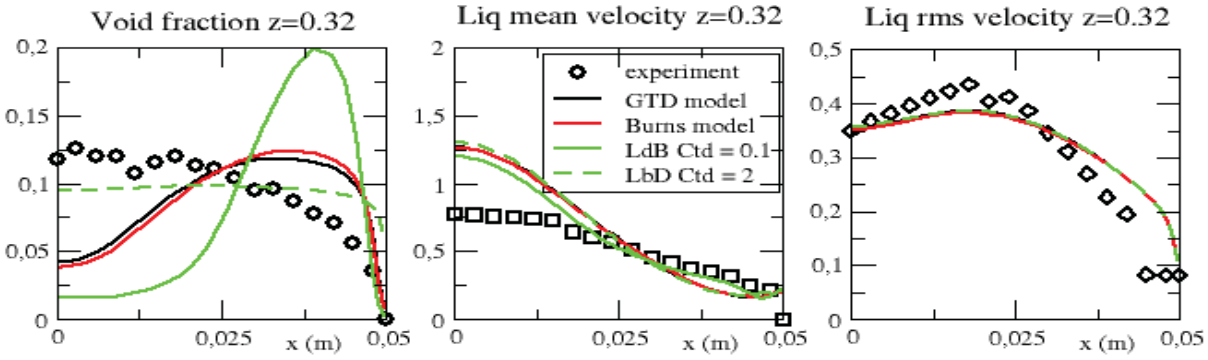

Figure 3-1.2 Bel F-dhila & Simonin experiment. Comparison of experimental data and NEPTUNE_CFD simulations for GTD, Burns and Lopez de Bertodano dispersion models.

In the experiment, bubbles migrate towards the center of the pipe. This phenomenon is under-estimated by numerical simulations, except for Lopez de Bertodano model using a large value for the constant. On the opposite, LdB model with the default value (0.1) increases the accumulation of bubbles near the wall.

3.1.3. CHAPTAL experiment:

The EDF CHAPTAL experiment [28] program intends to produce relevant experimental data of adiabatic bubbly flow, with hydraulic conditions close to pressurized water reactor operating range, for validation of NEPTUNE_CFD models. Indeed, at 10 bar, using water and Freon 116, the ratio of densities is equivalent to that of liquid water / steam at 90 bars (which allows us to approach the conditions in the reactor core 155 bars). Bubble diameter is, in contrast, not representative.
The mockup consists of a column of cylindrical sections of 38 mm inner diameter (d). The total height of the test section is 4.7 m (124d). The liquid mass flow rate is 2.271 kg/s. The corresponding Reynolds number is 125000. Details on the experiment and database can be found in [37].

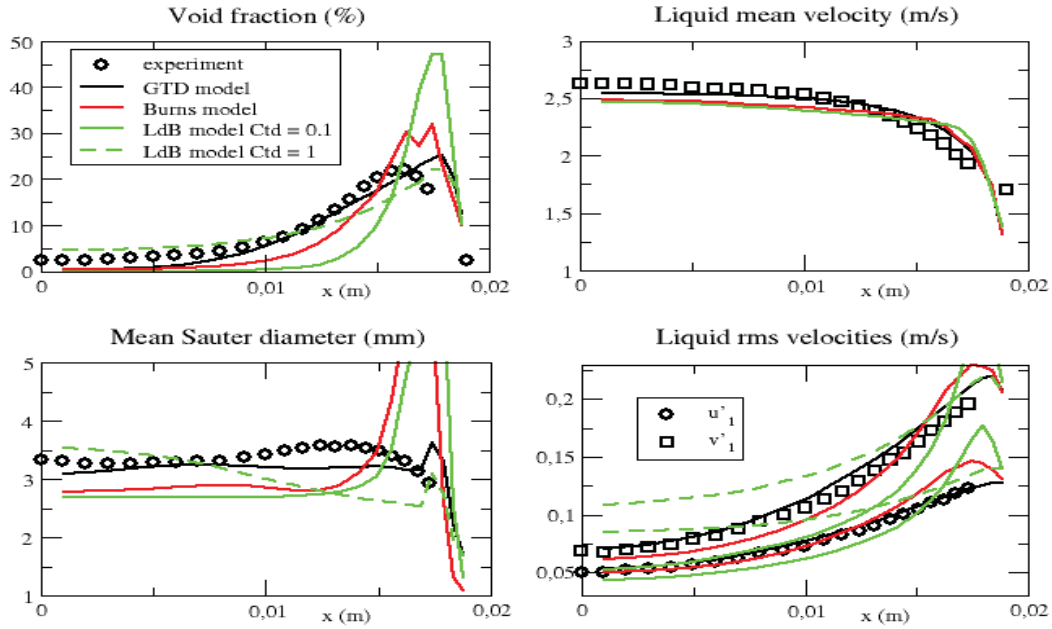

Figure 3-1.3a CHAPTAL experiment – gas mass flow rate = 0.014 kg/s. Comparison of experimental data and NEPTUNE_CFD simulations for GTD, Burns and Lopez de Bertodano dispersion models.

Figure 3-1-3a (3-1-3b resp.) presents comparisons for void fraction, Sauter mean diameter of bubbles, mean and fluctuating velocities for a low gas mass flow rate equal to 0.014 kg/ s (resp. high mass flow rate equal to 0042 kg/s). For both cases, the GTD model produces qualitatively encouraging results, compared to Burns model and LdB model. The last one using default Ctd value shows unrealistic void fraction and diameter peak: near the wall for low gas flow rate, in the core for high gas flow rate.
Furthermore it may be noticed that Burns model had some numerical instabilities for high void fraction.
Comparing to Liu-Bankoff and Bel F'dhila results, these preliminary simulations seem to show a larger sensitivity to the dispersion model choice when the fluid density ratio is close to PWR operating range

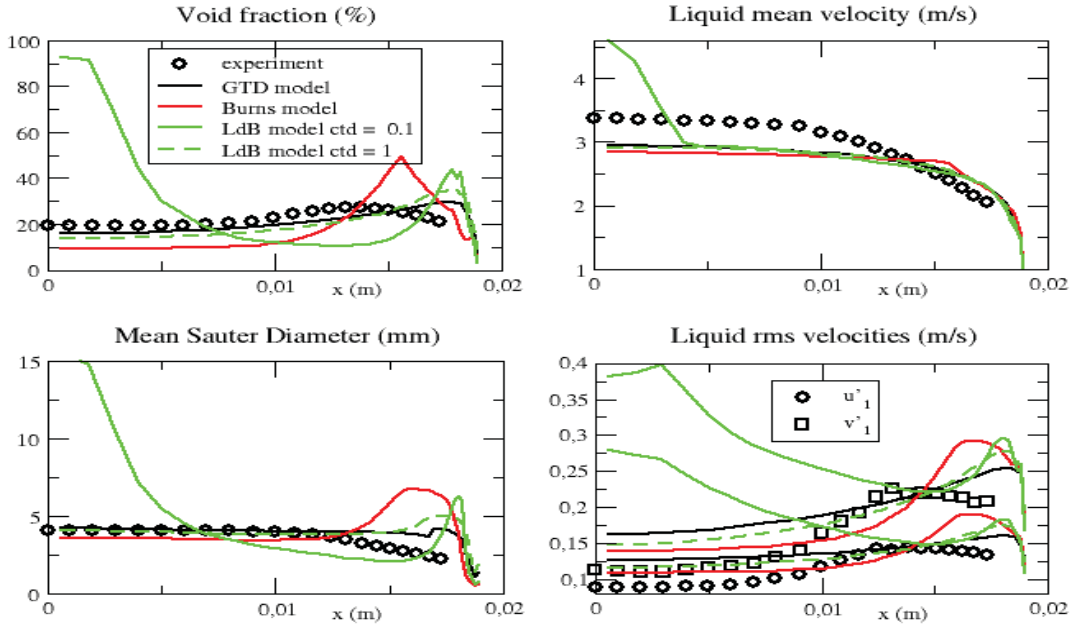

Figure 3-1.3b CHAPTAL experiment – gas mass flow rate = 0.048 kg/s. Comparison of experimental data and NEPTUNE_CFD simulations for GTD, Burns and Lopez de Bertodano dispersion models.

3.2. Liquid-steam boiling validation test-cases

3.2.1. ASU test-case

The Arizona State University experiment is described in [29] and [30] for two-phase boiling flow measurements. The test section of the ASU experiment consists of a vertical annular channel with a heated inner wall (diameter 15.9 mm) and an insulated outer wall (diameter 38.1mm). The inner tube is resistively heated, the upper 2.75 m of the 3.66 m long test section being the heated length. The lower 0.91 m serves as the hydrodynamic entrance length. The working fluid is a Freon R-113. The Reynolds number is around 17000. The measurement plane was approximately located at 1.94 m downstream of the beginning of the heated length.
Figure 3.2-1 presents comparisons for void fraction, liquid mean axial velocity and temperature. X axis denotes the radial coordinate (in m). An extra graph compares the turbulent dispersion coefficient obtained from the different models.
Globally, all three dispersion models present void fraction peak located far from the inner wall than in the experiment and an over-estimated peak of velocity. Secondly, numerical results of temperature and velocity seem to be non-sensitive to the model (as confirmed by the superposition of the curves), probably because Reynolds number is too low.

Finally, best results are obtained with LdB model using Ctd=2.

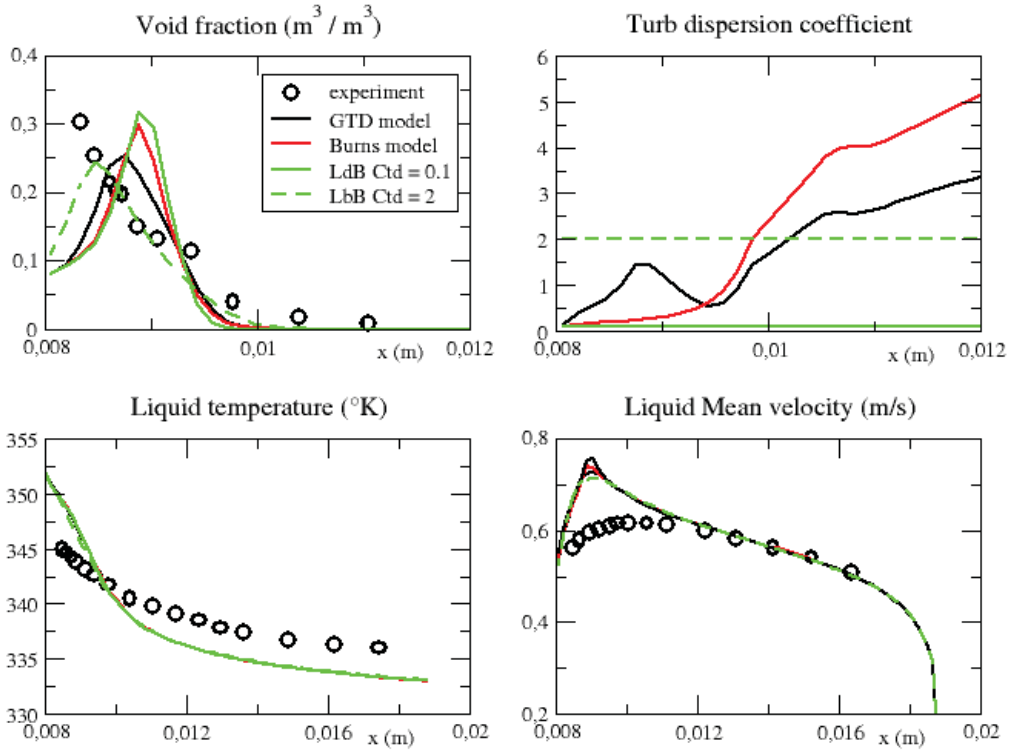

Figure 3-2.1 ASU experiment – Comparison of experimental data and NEPTUNE_CFD simulations for GTD, Burns and Lopez de Bertodano dispersion models.

3.2.2. TAMU test-case

This test facility was designed at the Texas A&M University [31] to investigate the sub-cooled boiling of fluid HFE-301 at low system pressure. The experiment was carried out in a rectangular vertical channel with a single heated wall. Particle Tracking Velocimetry (PTV) technique was used to measure time-averaged velocities and turbulence intensities. These experimental data allows investigate the validity of two-fluid turbulence models used for simulation of the boiling boundary region [32]. The fluid is pumped through a vertical, rectangular channel of length 530 mm. The dimensions of the cross section perpendicular to the flow are 8.7 mm by 7.6 mm. A heater with a length of 175 mm and a width of 7 mm is attached to one of the lateral walls of the channel 320 mm from the inlet, and provides heat fluxes up to 64 kW/m^2. The Reynolds number of the flow is about 16000.

Figure 3.2-2 presents comparisons for void fraction, liquid mean and rms axial velocity and liquid temperature. For sake of clarity, the rms profiles have been scaled by a factor of 2.

X axis denotes the radial coordinate (in m). An extra graph compares the turbulent dispersion coefficient obtained from the different models.

As in the ASU experiment, numerical results are non-sensitive to the dispersion model even if the associated coefficients are very different, which is probably a consequence of the low experimental Reynolds number.

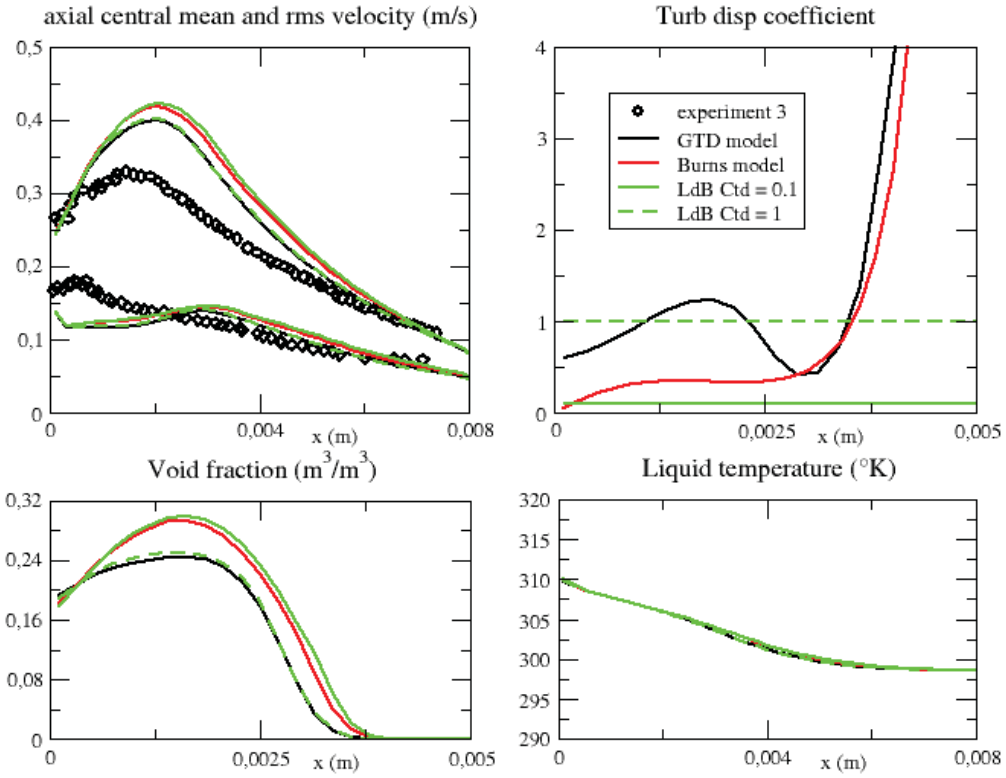

Figure 3-2.2 TAMU experiment – Comparison of experimental data and NEPTUNE_CFD simulations for GTD, Burns and Lopez de Bertodano dispersion models.

3.2.3. DEBORA test-case

This experiment, carried out at the CEA is devoted to the study of upward boiling bubbly flows in a vertical pipe with a circular cross section (Manon [11]). The sub-cooled working fluid, Freon R-12, is injected in the form of pure liquid at the bottom of the tube. The length of the pipe (5 m) can be divided into three successive parts: an adiabatic inlet length (1 m), a heated length (heated by Joule effect) equal to 3.5 m and an adiabatic outlet section (0.5 m). The measurement section is located at the end of the heated length and the internal diameter of the tube is equal to 19.2 mm. For the chosen case, the Reynolds number is about 300000.

Figure 3.2-3 presents comparisons for void fraction, gas axial velocity and liquid temperature.

The GTD model shows a good behavior for both quantities prediction, even if the void fraction profile is flatter than in the experiment.

On the opposite, Burns and LdB (Ctd = 0.1) models over-estimate the vapor production which tends to accelerate the liquid near the wall. In this area, the void fraction exceeds 80%, this value being close to classical CHF criteria. In other words, in this case these models cannot be used for the CHF detection.

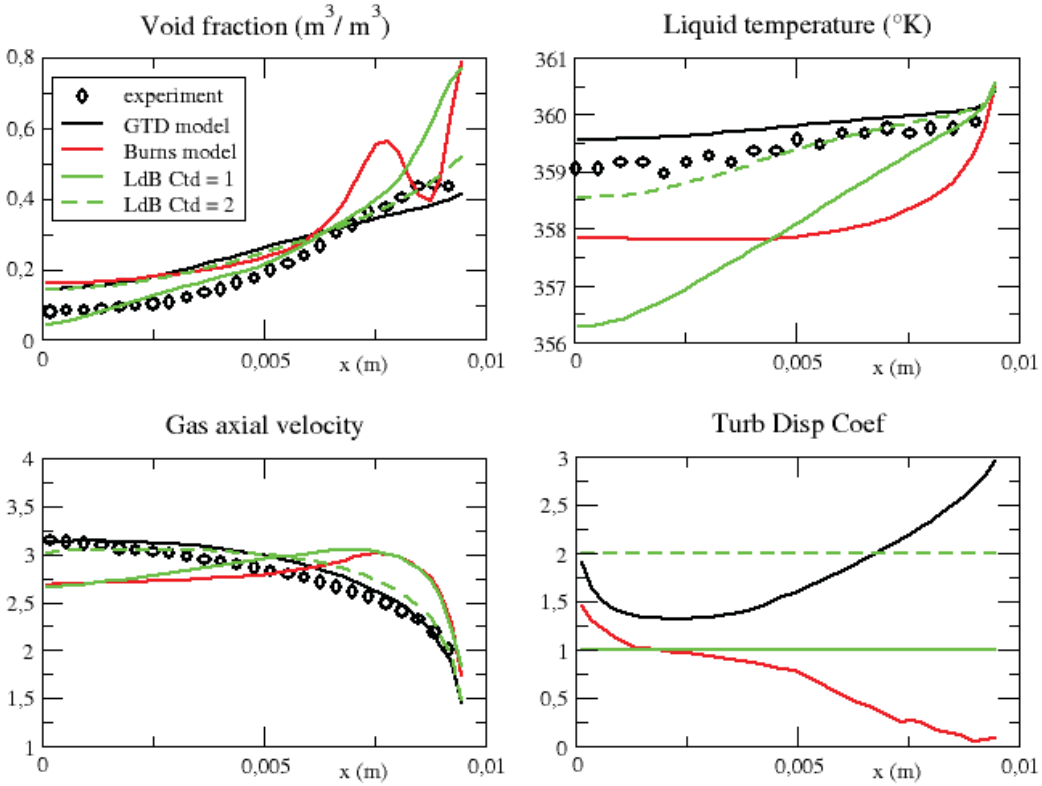

Figure 3-2.3 DEBORA experiment – Comparison of experimental data and NEPTUNE_CFD simulations for GTD, Burns and Lopez de Bertodano dispersion models.

3.2.4. Bartolomei test-case

This water-steam test case consists in the simulation of a non-equilibrium boiling flow as created by Bartolomei et al. [32]. Sub-cooled water is injected at the bottom of a vertical cylindrical tube with stepwise heating. The tube diameter is 12.03 mm, the heated section length is 1 m and the total tube length is L = 1.4 m. The outlet pressure is 70MPa and the inlet temperature around 500 K.

Cross section void fraction is measured over the tube length. In the heated lower section of the tube sub-cooled boiling occurs and steam is generated. The section above is adiabatic and vapor condensation occurs due to the mixing of the vapor generated near the heated wall in the lower section with the still sub-cooled liquid core.

Figure 3.2-4 presents comparisons for mean cross section void fraction, function of the height, for two conditions of inlet mass flow rate and wall heat flux.

As in the DEBORA test-case, GTD model correctly predict the void fraction evolution, while Burns model and Lopez de Bertodano model (Ctd=0.1) significantly over-estimate the void fraction.

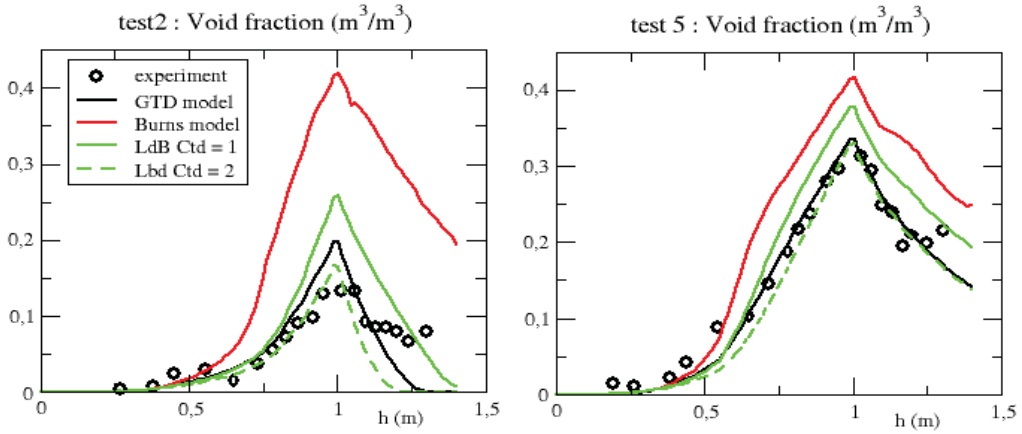

Figure 3-2.4 Bartolomei experiments – Comparison of experimental data and NEPTUNE_CFD simulations for GTD, Burns and Lopez de Bertodano dispersion models.

4. CONCLUSIONS AND PERSPECTIVE

One major objective of NEPTUNE project and a challenge for the NEPTUNE_CFD code is to get a reliable and robust modeling of turbulent water-steam bubbly–flow. Thus, the model used must be closed, validated and should not be based on user adjustments.

In this paper, we have presented in a first part the mathematical derivation of the turbulent dispersion force, namely the Generalized Turbulent Dispersion, which is one of the key points of the model. The closure for use in the two-fluid one-pressure Eulerian model was obtained by starting from a Lagrangian description of the two-phase flow. It takes into account local turbulent time scale and several momentum transfer coefficients of the flow and is user-parameters free.

In a second part, we have presented the comparison between numerical simulation and experimental data on a large test-case matrix, including adiabatic air-water flow and air-Freon flows, low Reynolds and high Reynolds boiling flows.
Three models are compared. One the one hand, Burn's model seems to be well-adapted for air-water flows, but over-estimates vapor production for high Reynolds number boiling flows. One the other hand, Lopez de Bertodano's model needs a change of the user parameter to be realistic on the whole range of flows. In the end, The Generalized Turbulent Dispersion model correctly reproduces the experiments, especially for flow regime close to PWR nominal conditions.

The major hypotheses that lead to this model derivation (low influence of liquid turbulence and mean velocity gradients) should nevertheless be revisited. Thus a more general model can be theoretically obtained from the derivation methodology adopted here, and then compared to experimental results.
While the GTD formulation does not depend on user-specified constants, a more important issue is the choice (user-choice) of drag, virtual mass and lift models that may contain their own empirical constants. These models have to be validated carefully, using for example simple analytic experimental data or two-phase Direct Numerical Simulation results.

ACKNOWLEDGMENTS

The NEPTUNE project is funded by EDF (Electricité de France), CEA (Commissariat à l'Energie Atomique et aux Energies Alternatives), AREVA-NP and IRSN (Institut de Radioprotection et de Sûreté Nucléaire).

REFERENCES

1. A. Guelfi, D. Bestion, M. Boucker, P. Boudier, P. Fillion, M. Grandotto, J.-M. Hérard, E. Hervieu, P. Péturaud, "NEPTUNE - A New Software Platform for Advanced Nuclear Thermal-Hydraulics", *Nuclear Science and Engineering*, **156**, pp 281-324 (2007).
2. S. Mimouni, F. Archambeau, M. Boucker, J. Laviéville, C. Morel, "A second order turbulence model based on a Reynolds stress approach for two-phase boiling flow. Part 1: Application to the ASU-annular channel case", *Nuclear Engineering and Design,* (2009).
3. S. Mimouni, F. Archambeau, M. Boucker, J. Laviéville, C. Morel, "A second order turbulence model based on a Reynolds stress approach for two-phase boiling flow. Part 1: Adiabatic cases", *Science and Technology of Nuclear Installations,* **792395**, 14 (2009).
4. S. Mimouni, F. Archambeau, M. Boucker, J. Laviéville, C. Morel, "A second order turbulence model based on a Reynolds stress approach for two-phase boiling flow and application to fuel assembly analysis", *Nuclear Engineering and Design,* **240**, pp. 2225-2232 (2010).
5. S. Mimouni, J. Laviéville, N. Seiler, P. Ruyer, "Combined evaluation of second order turbulence model and polydispersion model for two-phase boiling flow en application to fuel assembly analysis", *Nuclear Engineering and Design,* **241**, Issue 11 pp. 4523-4536 (nov 2011).
6. C. Morel, P. Ruyer, N. Seiler, J. Laviéville, "Comparison of several models for multi-size bubbly-flows on an adiabatic experiment", *International Journa of Multiphase Flow,* **36**, Issue 11 pp. 25-39 (Jan 2010).
7. M. Lopez de Bertodano, "Two Fluid Model for Two-Phase Turbulent Jet", *Nuclear Engineering and Design,* **179**, Issue 11 pp. 65-74 (1998).
8. A.D.B Burns, Th. Grank, I. Hamill, J.-M. Shi. "The Favre Averaged Drag Model for Turbulent Dispersion in Eulerian Multi-Phase Flows", *5th International Conference on Multiphase Flow, ICMF, Yokohama, Japan.* (2004)
9. M. Ishii, "Thermo-fluid Dynamics Theory of Two-Phase Flow, Eyrolles", Collection de la direction des Etudes et recherches d'Electricité de France (1975).
10. N. Méchitoua, M. Boucker., J. Laviéville, J.-M. Hérard, S. Pigny, G. Serre, "An unstructured finite volume solver for two-phase water/vapor flows modelling based on an elliptic-oriented fractional step method", *Proceedings of NURETH-10,* Seoul, (5-9 October 2003).
11. E. Manon, "Contribution à l'analyse locale des écoulements bouillants sous-saturés dans les conditions des Réacteurs à Eau Pressurisée", *PhD thesis, Ecole Centrale Paris* (2000)
12. E. Deutsch, O. Simonin, "Large Eddy Simulation applied to the motion of particles in Stationary Homogeneous Fluid Turbulence", *Turbulence modification in Multiphase Flows ASME,* Fed vol 110 pp. 35-42 (1991)
13. E. Deutsch, O. Simonin, "Large Eddy Simulation applied to the modelling of particulate transport coefficients in turbulent two-phase flows", *8th symposium on turbulent shear flows,*Tech. University of Munich (sept 1991)
14. J. Laviéville, E. Deutsch, O. Simonin, "Large Eddy Simulation of interactions between colliding particles and a homogeneous isotropic turbulence field", *Gas-Solid Flows ASME,* Fed vol 288 pp. 347-357 (1995)
15. P. Fede, G. Patino, O. Simonin, "Eulerian multiphase modelling of particle-particle and particle-turbulence interactions in polydisperse gas-solid flow". *Third International Conference on CFD in the Minerals Process Industries. CSIRO,* Melbourne, Australia, 10-12 (December 2003)
16. J-P. Minier, E. Peirano, "The PDF approach to polydispersed turbulent two-phase flows". *Physics Reports*, 352(1–3) pp. 1–214, (2001)
17. R. Gatignol. "The Faxén formulae for a rigid particle in an unsteady non-uniform Stokes flow". *Journal de Mécanique Théorique et Appliquée*, 1 (2) pp 143–160, (1983).

18. M. Ishii, N Zuber, “Drag Coefficient and Relative Velocity in Bubbly, Droplet or Particulate Flows”, *AIChE J.*, vol **25**, pp. 843-855, (1979)
19. A. Tomiyama, “Struggle with computational bubble dynamics”, *ICMF'98, 3rd Int. Conf. Multiphase Flow*, Lyon, France, pp. 1-18, (June 8-12, 1998)
20. P. Langevin. “Sur la Théorie du mouvement brownien“, *CR Acad. Sci. Paris*, 146(530-533), (1908).
21. G.T. Csanady, “Turbulent diffusion of heavy particles in the athmosphere”, *J. Atl. Sci*, **20**, pp. 201-208 (1963).
22. C.M. Tchen, “Mean value and correlations problems connected with the motion of small particles suspended in a turbulent fluide”, *PhD University of Delft*, The Hague (1947).
23. J.O. Hinze, “Turbulence”, *McGraw-Hill Book Company*, New York (1959).
24. Liu, T.J., Bankoff, G.: “Structure of air-water bubbly ow in a vertical pipe: I - Liquid mean velocity and turbulence measurements”, *Int. J. Heat Mass Transfer*, Vol. 36, 4, pp 1049-1060, (1993)
25. R. Bel F'Dhila, O. Simonin. “Eulerian prediction of a turbulent bubbly flow downstream of a sudden pipe expansion”, *Proc. 6th Workshop on Two-Phase Flow Predictions*, 30 mars-2 avril, Erlangen (EDF internal report HE-44/92.21, 1992).
26. R. Bel F'dhila, O. Simonin. “Eulerian Prediction of a Turbulent Bubbly Flow Downstream of a Sudden Pipe Expansion. Proc. 6th Workshop on Two-Phase Flow Predictions”, *Erlangen 1992, M. Sommerfeld (Editor), Bilateral Seminars of the International Bureau* / Forschungszentrum Julich GmbH, Vol. 14, pp 264-273, (1993).
27. R. Bel F'dhila, C. Suzanne, L. Masbernat, O. Simonin. “Local Measurement and Eulerian Prediction of a Turbulent Bubbly Flow Downstream of a Sudden Pipe Expansion”. *Experimental Thermal and Fluid Science*, Vol. 7, Issue 2, page 163, (1993).
28. P. Vasseur, “Rapport d'essais de la campagne 2012 du programme expérimental CHAPTAL Projet NEPTUNE lot 3.3“, *EDF Internal Report H-I84-2012-01909-FR* (2013).
29. A. Hassan, R.P. Roy., S.P. Kalra, “Experiments on subcooled ow boiling heat transfer in a vertical annular channel”, *International Journal of Heat and Mass Transfer*, vol 33, Issue 10, pp. 2285-2293 (1990).
30. R.P. Roy., V. Velidandla, S.P. Kalra, P. Péturaud , “Local measurements in the two-phase boiling region of turbulent subcooled C.E. Estrada-Perez , Y.A.Hassan, “PTV experiments of subcooled boiling flow through a vertical rectangular channel”, *Int. J. Multiphase Flow*, (2010).
31. B. Koncar, M. Matkovi, C.E. Estrada-Perez, Y.A. Hassan, “Numerical Simulation of Turbulent Subcooled Boiling Flow in a rectangular channel”, *Proceedings of the International Conference Nuclear Energy for New Europe*, Portoroz, Slovenia, (Sept. 6-9, 2010).
32. Bartolomei G.G., Batashova G.N., Brantov V.G., et al., “An experimental investigation of true volumetric vapour content with subcooled boiling in tubes” *Thermal Engineering*, vol. 29 (1982) pp. 132-135 (translated from Teploenergetika, no. 3, vol. 29, 1982, pp. 20-23)
33. P.A.Haynes, “Modeling of interfacial kinetic energy transfers for a turbulent bubbly flow”, *in proceedings of NURETH-7 conference,*Saratoga Springs (sept 1995).
34. P.A. Haynes, “Contribution à la modélisation de la turbulence pour les écoulements à bulles : proposition d’un modèle (k-eps) multi-échelles diphasique”, *Phd Thesis*, EDF Internal report, (2004).
35. R. Maxey, J. Riley, “Equation ot the motion of a small rigid sphere in a non-uniform flow”, *Phys. Fluids*, vol 26, n4, pp. 883-889 (1983).
36. E. Peirano, J.-P. Minier, "A probabilistic formalism and hierarchy of models for polysdispersed two-phase flows", *Physical Review E*, Vol. 65, 046301 (2002).
37. S. Mimouni, C. Baudry, M. Guingo, M. Hassanaly, J. Lavieville, N. Mechitoua, N. Mérigoux. "Combined evaluation of dynamics bubble, polydispersion model and turbulence modeling for adiabatic two-phase flows”, *in NURETH-16 proceedings*, 2015.
38. M. Lopez de Bertodano, R. T. Lahey, 0. C. Jones, “Phase distribution in bubbly two-phase flow in vertical ducts”, *Int. J. Multiphase Flow*, Vol. 20, p. 805, 1994